

# EXPERIMENTAL STUDY OF IGNITED UNSTEADY HYDROGEN JETS INTO AIR

J. Grune<sup>1</sup>, K. Sempert<sup>1</sup>, M. Kuznetsow<sup>2</sup>, W. Breitung<sup>2</sup>

<sup>1</sup>Pro-Science GmbH, Parkstrasse 9, Ettlingen, 76275, Germany, *surname@pro-science.de*

<sup>2</sup>Research Center Karlsruhe, P.O. Box 3640, 76021 Karlsruhe, Germany, *surname@iket.fzk.de*

## ABSTRACT

In order to simulate an accidental hydrogen release from the low pressure pipe system of a hydrogen vehicle a systematic study on the nature of transient hydrogen jets into air and their combustion behaviour was performed at the FZK hydrogen test site HYKA. Horizontal unsteady hydrogen jets with an amount of hydrogen up to 60 STP dm<sup>3</sup> and initial pressures of 5 and 16 bar have been investigated. The hydrogen jets were ignited with different ignition times and positions. The experiments provide new experimental data on pressure loads and heat releases resulting from the deflagration of hydrogen-air clouds formed by unsteady turbulent hydrogen jets released into a free environment. It is shown that the maximum pressure loads occur for ignition in a narrow position and time window. The possible hazard potential arising from an ignited free transient hydrogen jet is described.

## 1.0 INTRODUCTION

Hydrogen is already now being successfully used as energy carrier in motorized vehicles. The maintenance work that has to be carried out on the currently existing vehicles with "hydrogen technology" is performed by highly qualified experts in specific workshops. A broad introduction and further increase of the number of hydrogen powered vehicles will require a wide network of maintenance and servicing workshops. Due to the safety concept of the vehicles it is practically impossible that large amounts of hydrogen are released during the work in a servicing workshop. But if the depletion of the hydrogen supply line between tank and engine is performed incompetently or not at all, the release of smaller hydrogen amounts into the environment becomes possible during the maintenance work on the vehicle. Currently no systematic studies are available on the hazard potential of transient releases of small amounts of hydrogen with a subsequent ignition. In this study, the free jet release of hydrogen from pipes with residual overpressure is experimentally simulated. The main parameters in the experiments are: circular release opening with an inner diameter of 10 mm, initial reservoir pressures of 5 and 16 bar, and reservoir volumes of approx. 4, 10, 20 and 60 dm<sup>3</sup>. These parameters were derived from real dimensions of hydrogen supply systems in currently operated cars and busses. The free hydrogen jets will be ignited, and the resulting pressure and thermal loads to the environment will be investigated under variation of ignition position and ignition time-point. Goal of this work is to quantify the possible hazards arising from ignited free transient hydrogen jets, to allow an evaluation of the fire and explosion hazard in workshops due to hydrogen releases.

## 2.0 EXPERIMENTAL SET-UP

The facility for the generation of a defined and transient horizontal hydrogen jet from a pressure reservoir with a residual overpressure is shown in Figure 1.

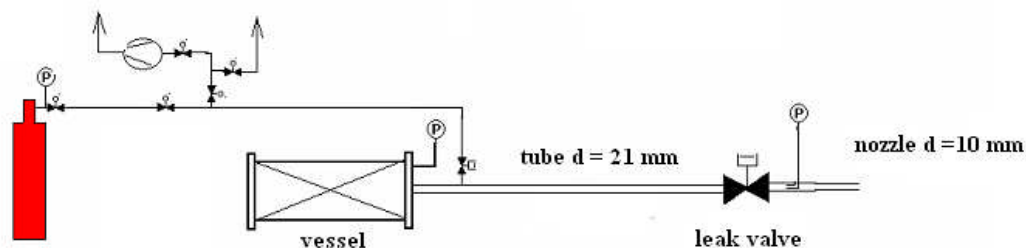


Figure 1: Schematic of the facility for transient hydrogen release from a pressurized reservoir.

It consists of a system of pipes with a small valve for the hydrogen filling procedure and a large valve ( $d_i = 21$  mm) for the hydrogen release. The pipe system has a total volume of  $0.25$  dm<sup>3</sup> and thereby acts as the smallest vessel F (see Table 1). With the installation of additional pressure vessels A – E, the required vessel volumes and released hydrogen amounts were reached for the two pressure stages of interest.

Table 1: Initial conditions of hydrogen release to the ambient atmosphere.

Vessel type	Volume (dm <sup>3</sup> )	H <sub>2</sub> released at 5 bar STP dm <sup>3</sup>	H <sub>2</sub> released at 16 bar STP dm <sup>3</sup>
F	0,25		3,75
E	0,8	3,2	12
D	1,25	5	18,75
C	2	8	30
B	4	16	60
A	12	48	

Since the nominal diameter of the ball valve used in the leak is larger than the cross section of the nozzle, short leakage opening times (5 ms) can be reached. With pressure measurements in the vessel and in the nozzle element the hydrogen release and the leakage opening time are registered. Figure 2 shows the details of the welded nozzle element used for the hydrogen release.

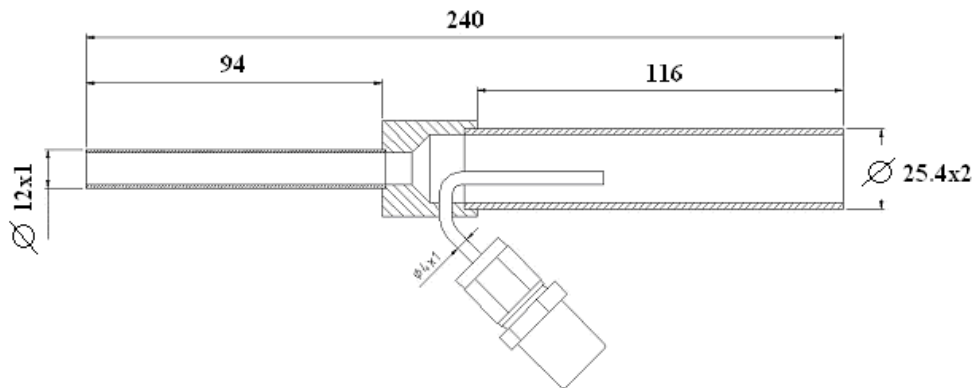


Figure 2: Nozzle element of the test facility.

The experiments were performed in a specific test chamber of the hydrogen test site of the Institute for Nuclear and Energy Technologies (IKET) on the premises of the Karlsruhe Research Centre (FZK). This test chamber encloses a volume of approx.  $160$  m<sup>3</sup>. The experimental facility was mounted on a rack (I. in Fig. 3) so that the axis of the H<sub>2</sub>-jet had an unobstructed length in space of  $4$  m and a distance to the floor and the nearest wall of  $1.6$  m. The jet axis (III. in Fig. 3) and the nozzle exit (II. in Fig. 3) are the major reference points for the positions of the ignition source and the sensors used. As ignition source a high frequency electric arc ( $20$  kHz,  $\sim 60$  kV) with an electrode distance of  $\sim 6$  mm was used. The thermal power of the spark system is approx.  $10$  W. The electrodes were positioned along the jet axis via a lance (IV. in Fig. 3), the distance between the ignition lance and the nozzle exit is adjustable via a sledge. Five dynamic pressure sensors (PCB Type 113A31) were used for the pressure measurements. These pressure sensors were mounted in special adapters and positioned in a line with a distance of  $40$  cm to each other (V. in Fig. 3). This pressure sensor line was used in parallel or perpendicular orientation to the jet axis in the experiments. In the configuration parallel to the jet axis depicted in Fig. 3 reflected pressures were measured. In a large number of experiments two heat flux sensors were positioned via lances along the jet axis (VI. in Fig. 3). Due to the density gradients of the H<sub>2</sub>-jet shadow phenomena occurred in the experiments and were recorded by a high speed camera. A  $5$  kW floodlight lamp was used to project the jet on a screen behind the rack.

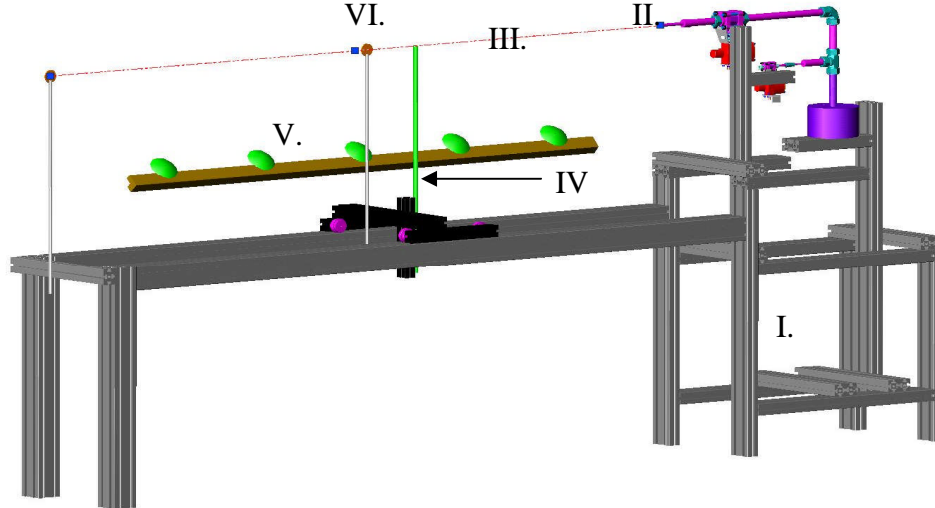


Figure 3: CAD-drawing of the experimental set-up.

First it is necessary to evaluate the dynamics of H<sub>2</sub>-releases from the pressurized vessels. The effluent formula of SAINT-VENANT and WANTZELL [1] (eq.1) describes the effusion velocity  $c_2$  of a gas from a vessel in dependence of the undisturbed gas state  $P_1$  and  $T_1$  in the vessel under the assumption of an ideal frictionless nozzle flow.

$$c_2 = \sqrt{2 \left( \frac{\kappa}{\kappa - 1} \right) \frac{P_1}{\rho_1} \left[ 1 - \left( \frac{P_2}{P_1} \right)^{\frac{\kappa - 1}{\kappa}} \right]} \quad (1) \quad \Delta m(t) = \frac{1}{\phi} \cdot c_2(t) \cdot \rho_1(t) \cdot A_{Nozzle} \cdot \Delta t \quad (2)$$

where  $P_1$  - pressure inside vessel;  $P_2$  - pressure outside vessel;  $\rho_1$  - density inside vessel;  $\kappa$  - adiabatic exponent;  $\Delta m$  - mass release in time step  $\Delta t$ ;  $A$  - nozzle area;  $\phi$  - nozzle form factor.

With the introduction of a small time step  $\Delta t$ , during which the gas effuses with the velocity  $c_{2(n=0)}$ , a new initial state  $P_{1(n=1)}$  with the effusion velocity  $c_{2(n=1)}$  can be calculated using the nozzle cross section (eq.2) and the vessel volume. The number  $x$  of the calculation steps  $n$ , until the ambient pressure is reached by the state  $P_{1(n=x)}$ , determines the ideal effusion time. With this calculation method the transient effusion is approximated by a sequence of quasi stationary states. Compared with the ideal case, temperature effects and a friction afflicted gas flow in complex nozzle geometry with different tube diameters and an opening ball valve are present in reality. The deviation of the real H<sub>2</sub>-release rate from the ideal case is described here by a nozzle form factor  $\phi$  (eq.2). For the vessels A – E nozzle form factors of approx. 2 were experimentally determined, for the smallest vessel F a  $\phi$ -value of ~3.5 was found. In Figure 4 the time dependence of the pressure inside vessel B [4 dm<sup>3</sup>] during the effusion process is shown. The comparison of the measured pressure curves with the calculated ones using the equations 1 and 2 shows a very good agreement for the initial pressures of 5 and 16 bar. For both calculated curves in Figure 4 a nozzle form factor of 2.2 and a valve rotation time of 5 ms were used. The shape of the pressure histories of all vessels investigated is similar at the same initial pressure. With the balance condition that the pressure drop inside the vessel is equivalent to the released mass of hydrogen, very high mass flows are observed for a short time after the valve is completely opened. Figure 4 (right) shows the hydrogen mass flow history through the 10 mm tube nozzle for initial pressures of 5 and 16 bar for vessel B. At an initial pressure of 16 bar the maximum release rate is calculated to be 97 g/s.

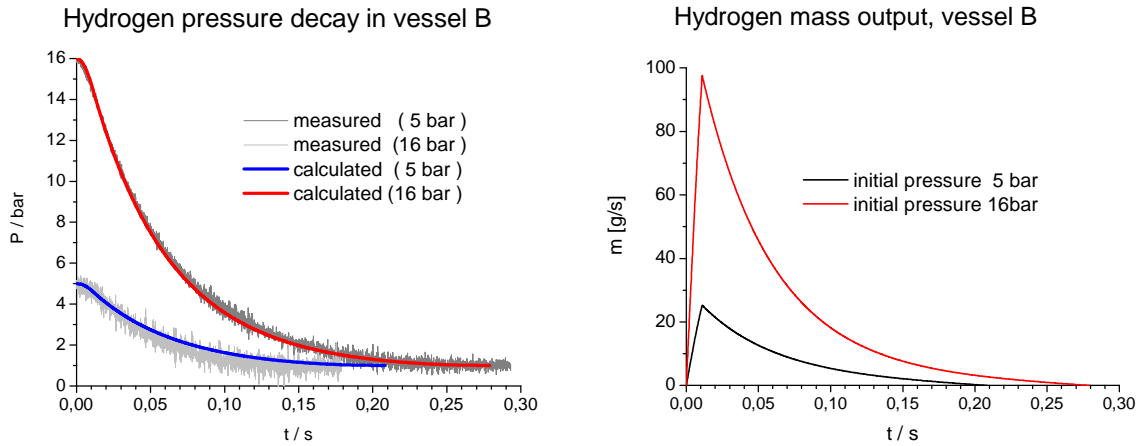


Figure 4: Left: Measured and calculated pressure decay in vessel B. Right: Hydrogen mass output in g/s through the 10 mm tube nozzle for vessel B, calculated for isothermal conditions.

### 3.0 EXPERIMENTAL RESULTS FOR IGNITED UNSTEADY FREE JETS

Due to the high initial effusion velocity of the hydrogen from the nozzle the influence of gravity is negligible. In Figure 5 two typical movie sequences of combustion experiments are depicted. The sequence on the top (from left to right) shows an experiment with vessel D16 [ $1.25 \text{ dm}^3$ ;  $P = 16 \text{ bar}$ ; release of  $18.75 \text{ dm}^3 \text{ H}_2$ ] and early ignition close to the nozzle.

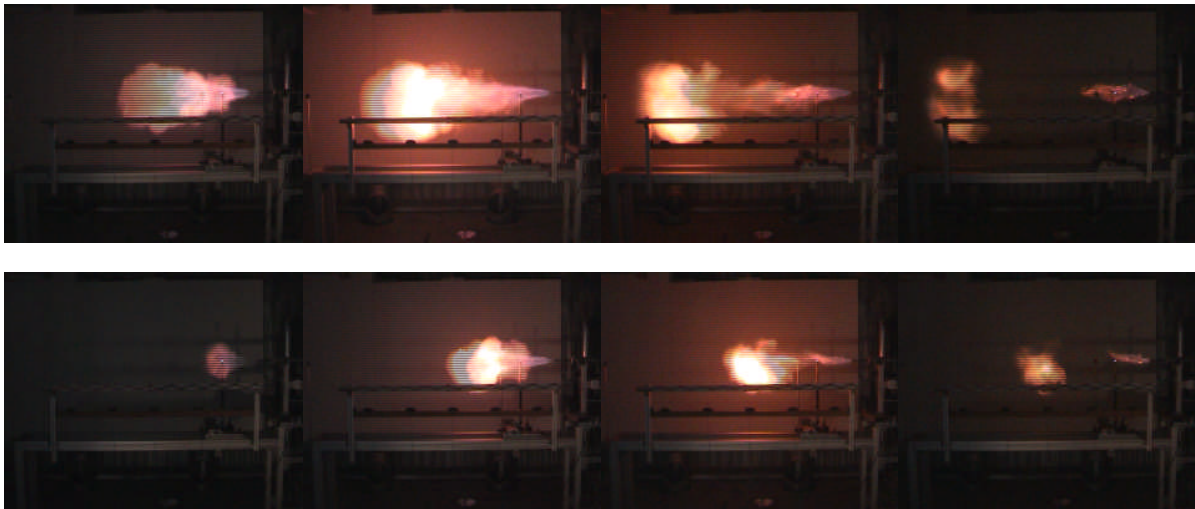


Figure 5: Sequences from digital videos. Top: vessel D16 [ $1.25 \text{ dm}^3$ ;  $P = 16 \text{ bar}$ ]. Bottom: vessel D5 [ $1.25 \text{ dm}^3$ ;  $P = 5 \text{ bar}$ ].

In the sequence below an experiment with vessel D5 [ $1.25 \text{ dm}^3$ ;  $P = 5 \text{ bar}$ ; release of  $5 \text{ dm}^3 \text{ H}_2$ ] with early ignition close to the nozzle is depicted. In both sequences the time step between two images is 40 ms. From these images, taken with a standard digital video camera, only qualitative statements can be derived, since the point in time of the first frame with a visible flame is not defined. The injected  $\text{H}_2$  – air cloud burns out from the right (ignition location) to the left (edge of burnable cloud). In the images a symmetrical distribution of the flame relatively to the horizontal jet axis can be recognised. A comparison of the two sequences shows geometrical similarity concerning the shape of the flame propagation.

### 3.1 Effect of the ignition position and time delay on the amplitude of the pressure wave

The dynamics of the hydrogen jet burn out can be determined using the shadow-schlieren images. Plotting the ignition positions on the jet axis against delayed time for the first possible ignition produces a distance-time-diagram for the ignitable hydrogen front as shown in the left graph of Figure 6. Mean velocities of the leading flammable hydrogen front (cloud) are plotted against the distance to the nozzle for different vessels and initial pressures in the right graph. For medium and large vessels the mean axial velocity of the flammable hydrogen cloud at a distance of 50 cm to the nozzle amounts to approx. 50 to 60 m/s. With increasing distance from the nozzle this velocity decreases. When the horizontal propagation velocity of the flammable hydrogen front approaches zero, the distance is reached at which the released hydrogen can no longer be ignited. In case of an ignition at a position far from the nozzle on the jet axis, in a region with low velocities of the flammable hydrogen front, only a small fraction of the released hydrogen is burned.

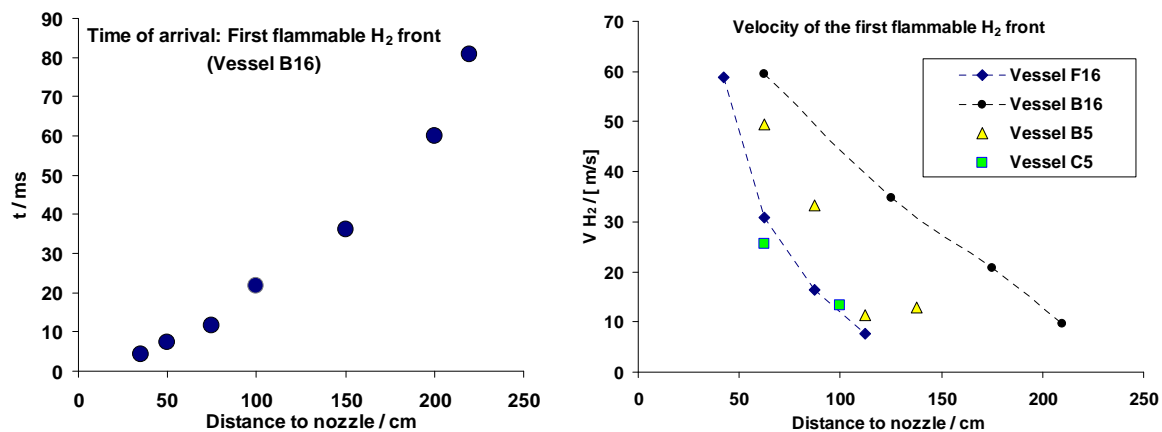


Figure 6: Left: Arrival time of the first flammable hydrogen front (vessel B; P = 16 bar). Right: Mean velocity of the first flammable hydrogen front on the jet axis.

In experiments with ignition positions close to the nozzle it was observed, that the hydrogen jet could not be ignited by an early ignition spark on the jet axis, since the local hydrogen concentration in the leading front lies above the upper flammability limit under these conditions. With the transient decrease of the hydrogen mass flux during the effusion process the hydrogen concentration falls below the upper flammability limit and the mixture becomes ignitable later in time. In the experiments it was found that an ignition time at which the leading hydrogen front had already passed the ignition position may cause a detectable pressure wave. In Figure 7 the influence of the ignition time and the ignition position on the maximum pressure wave amplitude is shown for vessel B ( $P_0 = 16$  bar) as an example. The injected hydrogen volume in this case is  $60 \text{ STP dm}^3$ . The graphs show the dependence of the peak overpressure on the ignition time for four different ignition positions. The location of the pressure sensors is depicted on the right side of Figure 7. The distance between the jet axis and the pressure-transducers-lance was 50 cm. The recorded overpressures are reflected pressure values. With a near ignition at a distance of 35 cm to the nozzle a combustion with moderate overpressure generation at approx. 5 ms after the leak opening is possible (compare Figure 6 left). A noticeable increase of the overpressure is observed with an increase of the ignition delay time by 4 ms to then 9 ms. The sensors close to the ignition position show the highest pressures. In the ignition time span from 9 ms to 57 ms the released hydrogen is not ignitable at a distance of 35 cm from the release nozzle in the experiments, presumably because the hydrogen concentrations in this area are above the upper flammability limit. After 57 ms the release rate has decreased to such an extent, that a flammable mixture is present at the 35 cm position. In this ignition situation the highest overpressures were detected by the sensors near the ignition. With an ignition distance of 50 cm (Figure 7 top right) the maximum pressure peaks are generated for ignitions between 20 ms and 40 ms after the beginning of the effusion process.

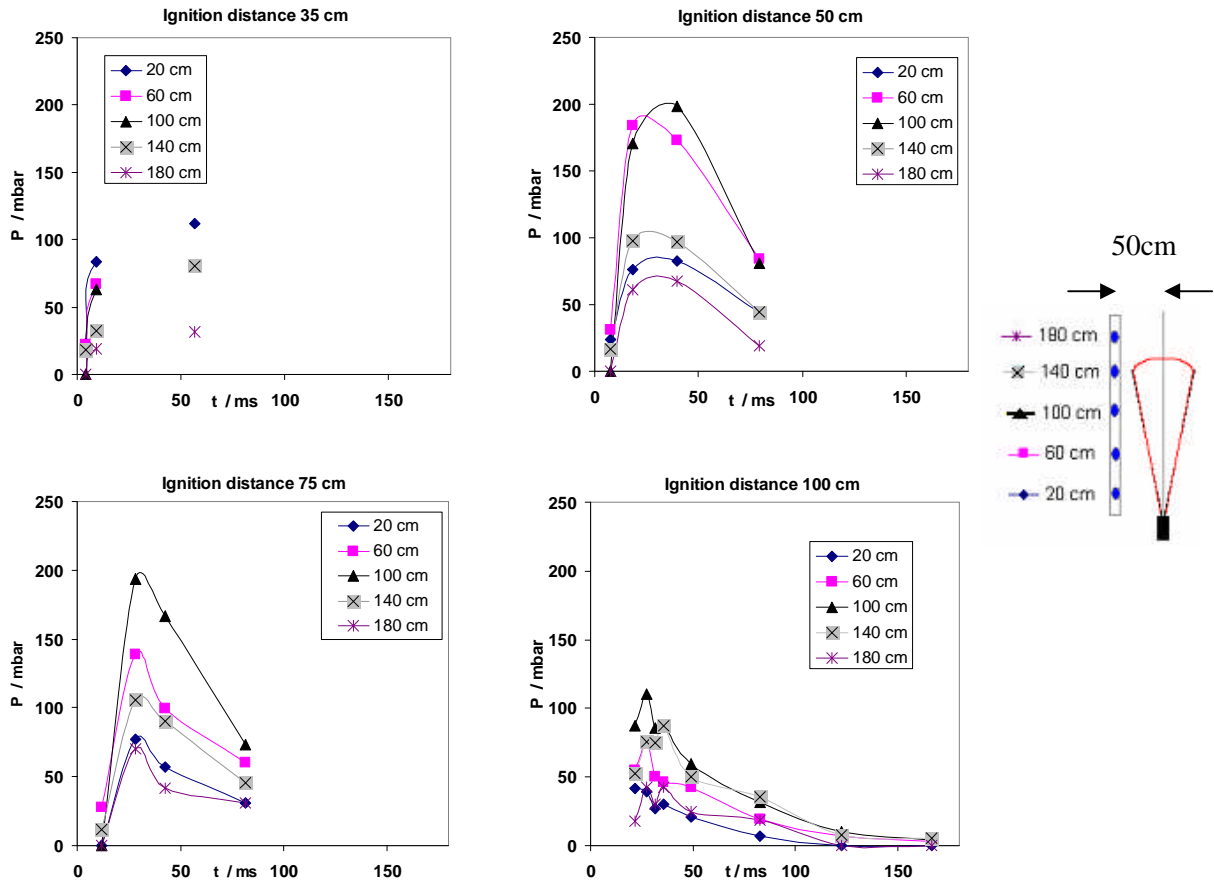


Figure 7: Vessel B ( $P_0 = 16$  bar); dependency of the maximum overpressure on the ignition time and the ignition position. The legend shows the distance of the pressure transducers from the nozzle and the jet axis (right sketch).

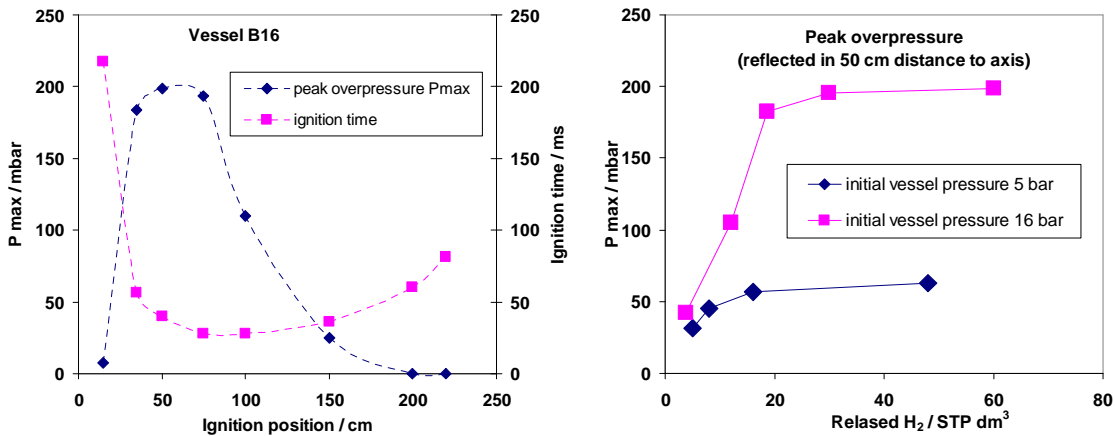


Figure 8: Left: Vessel B ( $P_0 = 16$  bar); determination of the ignition time window and the ignition position for maximum amplitudes of the pressure wave. Right: Measured maximum reflected overpressures as function of the effused hydrogen amount.

With an ignition distance of 75 cm similar pressure amplitudes are reached at an ignition delay time of 30 ms. For an ignition distance of 100 cm systematically lower pressure amplitudes are measured. In the left graph of Figure 8 the maximum overpressures for vessel B16 are depicted as function of the



ignition position, independent of the pressure sensor location. On the left ordinate the maximum overpressure and on the right ordinate the corresponding ignition time is given, for which the maximum overpressure was measured. The left plot of Figure 8 demonstrates that for vessel B16 the ignition in a small time window (~30 to 50 ms) and a corresponding small range of the ignition position on the jet axis (between 35 and 75 cm) leads to combustions with high pressure development. For all vessels and initial pressures investigated similar ignition time windows and positions for the generation of maximum overpressures were observed. Considering the small effusion times of the hydrogen from the different vessels, very narrow time windows and ignition distances exist which lead to a combustion with maximum possible pressure amplitude, especially for small and medium vessels. In the right side of Figure 8 the measured maximum overpressures during the experiments with the pressure sensor line oriented parallel and perpendicular to the jet axis are plotted against the released total amount of hydrogen in  $\text{dm}^3$ . With the assumption that the pressure wave propagates with constant speed of sound and due to the linear orientation of the pressure sensors it is possible to determine the origin of the pressure wave using the different arrival times of the wave at the sensors. This location is found approx. 10 cm behind the ignition position, immediately ( $< 1\text{ms}$ ) after the ignition. The image series in Figure 9 shows the ignition sequence of a combustion experiment with vessel B ( $P_0 = 16\text{ bar}$ ) at an ignition distance of 50 cm. The image series starts 1 ms before the initiation of the ignition by an ignition spark. The first image shows the flow of hydrogen. On the next pictures the visibility of the hydrogen flow is enhanced by means of digital image processing. The ignition of the hydrogen cloud takes place between the second and third picture. The propagation of the flame front is shown in the following images. Using frame 2 (1 ms) and 3 (2 ms) a mean flame velocity of approx. 450 m/s can be estimated. Between the images 3 (2 ms) and 4 (3 ms) the flame propagates in the direction of the flow with a mean velocity of approx. 200 m/s. Between the last two frames of the series (4 ms and 6 ms) the mean flame velocity in flow direction, averaged over two milliseconds, amounts to only approx. 80 m/s. The short period with high burning velocity (local explosion) of the turbulent hydrogen free jet is illustrated in higher resolution in Figure 10.

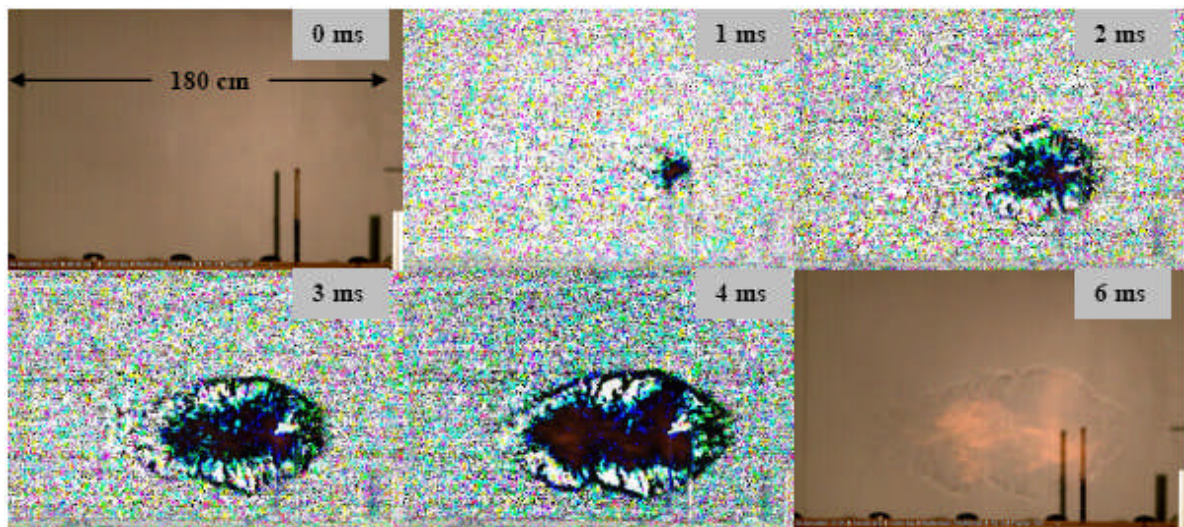


Figure 9: Vessel B ( $P_0 = 16\text{ bar}$ ); ignition position 50 cm, ignition time 41 ms after leak opening.

The picture series of Figure 10 is taken from a high speed movie. It starts with the first visible burning spot which is observed about 10 cm behind the ignition lance (dark vertical line). The spread of the transient jet and the following flame propagation is visible as shadow. The scale in the first picture relates to the shadow screen. In addition the real hydrogen flame is visible as light coloured area. A near spherical flame propagation from the first visible spot takes place. In the flow direction of the jet the flame velocity is higher than the sonic speed in air. The short period (Fig.10) with high burning velocity (local explosion) of the turbulent hydrogen free jet, which is close to the speed of sound of the unburned gas mixture, generates the pressure wave.

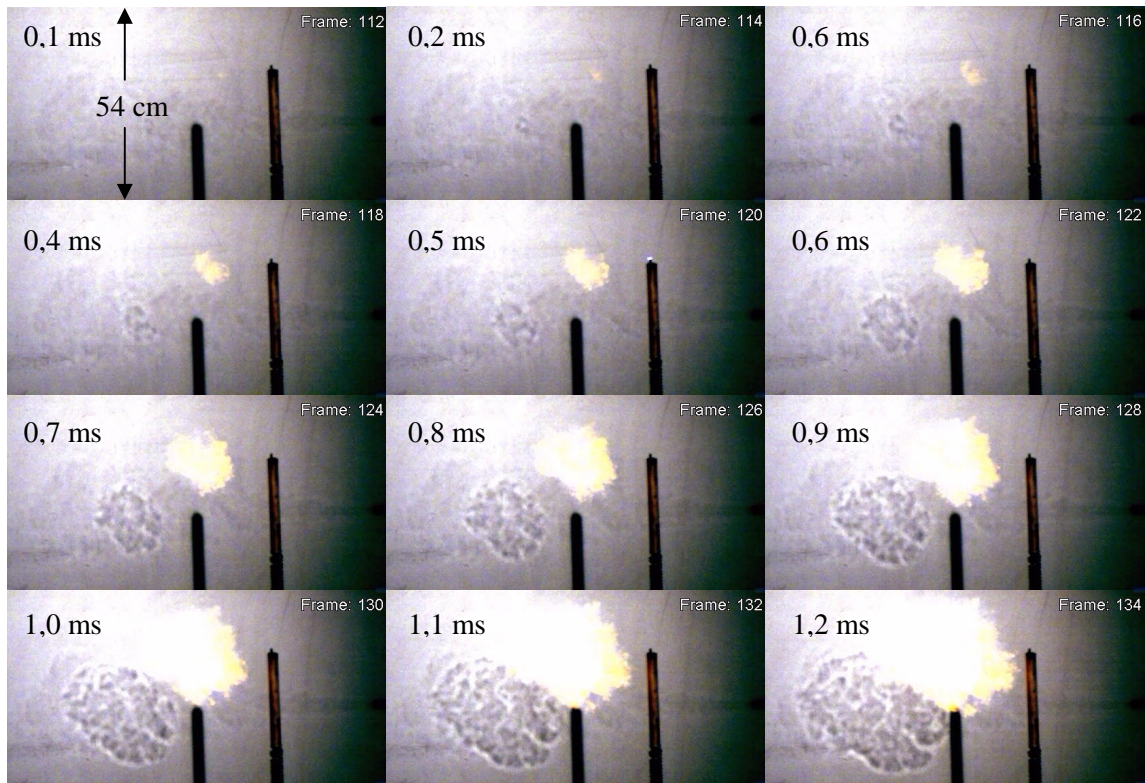


Figure 10: High speed movie of the jet ignition during the period of high burning velocity. Vessel B ( $P_0 = 16$  bar); ignition position 50 cm, ignition time 41 ms after leak opening.

### 3.2 Maximum amplitudes and propagation of the pressure waves

The maximum overpressures plotted in the right side of Figure 8 were measured in reflected orientation and in a distance of 50 cm to the jet axis. To avoid the influence of reflections and to describe the spatial propagation of the pressure wave the pressure sensor line was positioned also perpendicular to the jet axis, in a way that allows the pressure wave to pass the sensors. In Table 2 the values for the parameters ignition position and ignition time leading to maximum pressure waves are listed. Additionally the distance of the perpendicularly oriented pressure sensor line to the jet nozzle is specified in this table.

Table 2: Ignition position, ignition time (after leak opening) and the distance of the perpendicularly oriented pressure sensor line from the nozzle.

Vessel	Ignition position / cm	Ignition time / ms	Pressure sensor line / cm	Vessel	Ignition position / cm	Ignition time / ms	Pressure sensor line / cm
B16	50	41	60	A5	50	39	60
C16	50	25	60	B5	25	39	35
D16	50	16	60	C5	25	27	35
E16	50	26	60	D5	50	16	60
F16	35	18	45				

In Figure 11 typical pressure signals, measured in a distance of 80 cm to the jet axis with non-reflecting orientation of the pressure sensors, are shown. The experimental parameters ignition time and ignition position can be found in Table 2. The recorded pressure signals of the combustion experiments with the vessels D5 to B16 show no significant differences concerning the duration of the



pressure waves. For all pressure signals analysed a mean duration of the positive waves of 1.5 ms was determined.

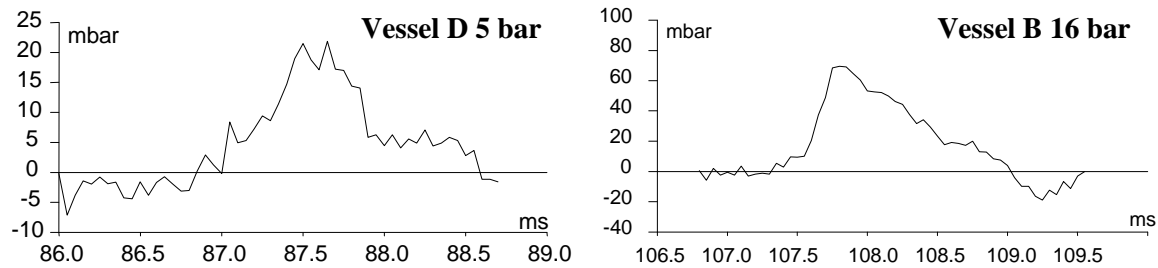


Figure 11: Pressure signals from the transient recorder; distance 80 cm to the jet axis, ignition time and ignition position according to Table 2.

Plotting the measured amplitudes of the pressure waves against the reciprocal distance to the jet axis produces approximately linear relations for all vessels investigated, which would be typical for a cylindrical pressure source with  $1/r$  dependence.

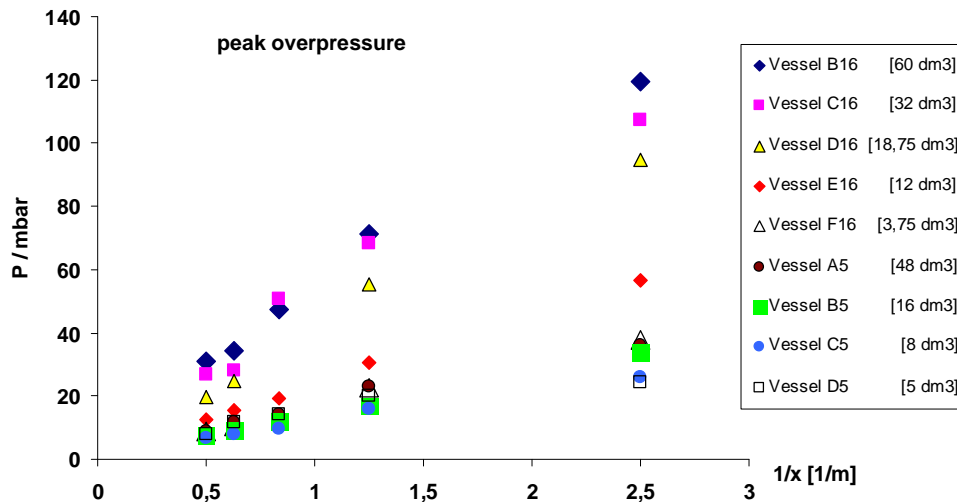


Figure 12: Measured maximum overpressures as a function of the reciprocal distance to the jet axis. (Side-on pressure transducer orientation).

### 3.3 Thermal energies from the ignited hydrogen release

If the experimental facility for hydrogen releases used in this work is considered as a transient turbulent diffusion burner, approx.  $10.75 \text{ kJ/dm}^3$  [ $120 \text{ kJ/g}$ ] of thermal energy could be released in case of a complete combustion of the hydrogen released from the vessels. It can be assumed that the thermal energy release follows the mass output curve (Fig. 4) with some time shift. At an initial pressure of 16 bar the theoretical thermal peak power of the transient diffusion burner would amount to 11.6 MW, at an initial pressure of 5 bar it would be still 2.8 MW. So the question arises about the thermal loads on objects in the vicinity of the burning free jet. For measurements of the transmitted thermal energy of the ignited transient  $\text{H}_2$ -free jet, copper disks were positioned as heat flux sensors at different positions along the jet axis in the experiments. With a suitable dimensioning of the surface-to-mass ratio of the copper body, high temperatures inside the gauge body can be avoided, and a high heat transfer is provided. Using the heat capacity  $C_p$ , the mass  $m$  and the surface  $A$  of the copper disk, with measurements of the temperature difference  $\Delta T$  inside the copper body a time integrated heat flux for the heat exposure time from  $t_0$  to  $t$  in  $\text{kJ/m}^2$  can be calculated. As sensor bodies copper disks with a diameter of 50 mm, a thickness of 2 mm and a mass of 30 g were used. The temperature of the disks was measured via thermocouples in the centre of the disk. Since the total heat of the hydrogen

combustion was estimated in a range from 34.4 kJ to 645 kJ, the high power described before is only released for a very short time. A significant thermal radiation of the ignited transient free jets was not observed in the experiments, so the measurements conducted concentrated on the axis of the hydrogen jet. The data plotted against the jet axis in Figure 13, show a multitude of measured integral heat fluxes from the combustion experiments with three different vessels. In the experiments the ignition time was varied for different ignition positions. The left graph in Figure 13 shows an approximately linear decay of the measured maximum heat fluxes for the different vessels with increasing axial distance from the nozzle. The measured integral heat fluxes exhibit a strong correlation with the amount of hydrogen released. In the heat flux density measurements on the jet axis in a far distance to the nozzle (250 cm) it was observed that a maximum axial propagation of the burnt gases occurs at ignition positions between 50 and 100 cm on the jet axis. The right side graph of Figure 13 shows the measured heat fluxes on the jet axis in a distance of 250 cm from the nozzle as function of the ignition position of the released hydrogen for different vessels. An early ignition of the released hydrogen close to the nozzle generates the highest thermal loads.

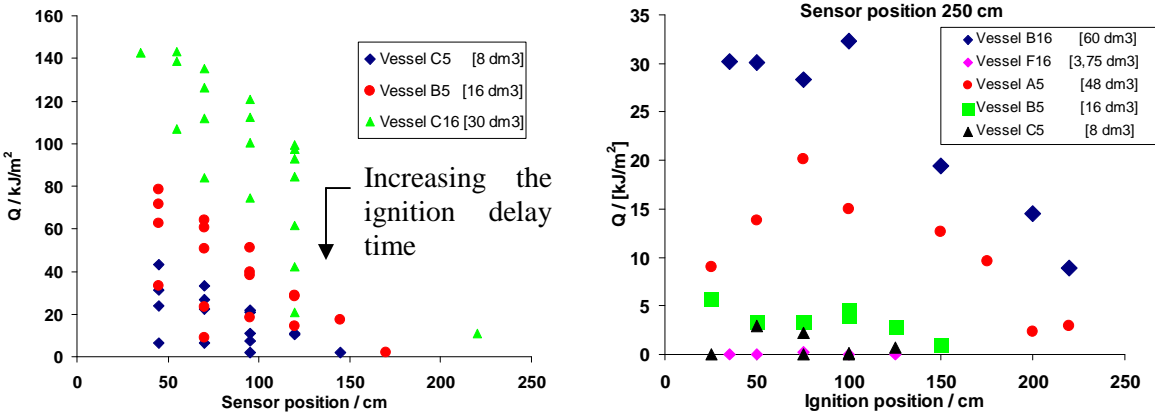


Figure 13: Left: Measured maximum integral heat fluxes along the jet axis. Right: Measured heat fluxes on the jet axis in a distance of 250 cm to the nozzle.

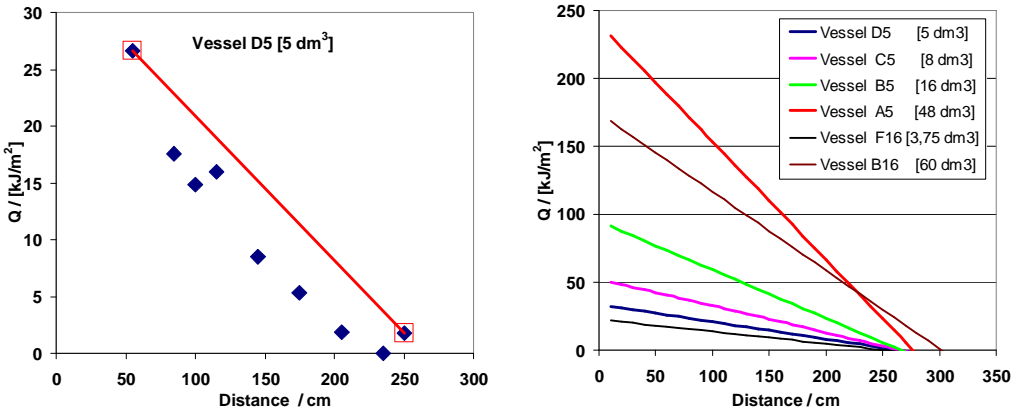


Figure 14: Left: Linearization of the maximum possible thermal loads on the jet axis as a function of the distance to the nozzle. Right: Estimation of the maximum possible thermal loads on the jet axis for different vessels.

In a larger distance to the nozzle, close to the maximum thermal ranges of the ignited hydrogen jets, for different ignition positions different thermal loads are measured. A bounding straight line can be drawn in these graphs, on or below which all measured data points are located, Figure 14 left. The conservative linearization of the possible maximum thermal loads on the jet axis in Figure 14 is not valid for the region close to the nozzle. In this region no measurements were performed. The point of

intersection of the straight lines in Fig. 14 with the abscissa can be considered as the maximum thermal range of the ignited free jet, which is quite considerable between 2.5 m and 3 m.

## 4.0 HAZARD POTENTIALS

### 4.1 Hazard potential from pressure loads

The combustion experiments have shown that the hydrogen effusing as free jet is quickly diluted with air. The time span in which the gas cloud is ignitable is almost identical with the effusion time of the gas from the vessels. For many ignition times and ignition positions the ignition of the unsteady free jet produced only a local combustion with no detectable pressure wave. In contrast to this, an ignition of the free hydrogen jet shortly after it has reached its maximum effusion rate can lead to a local explosion with detectable pressure waves. The maximum measured amplitudes of the pressure waves for the vessels investigated in experiments with initial pressures of 5 bar and 16 bar are plotted against the distance perpendicular to the jet axis in Figure 15. In this graph the lower thresholds for a possible damage of the ear-drum at exposure durations of the positive peak overpressure of 1 and 2 ms, according to [2], are also depicted for comparison. The mean duration of the positive pressure phase determined in the experiments amounted to about 1.5 ms for all vessels and initial pressures investigated. For further orientation on the hazard potential of pressure waves the thresholds of overpressure amplitudes are depicted, above which window glass breakage may occur [3].

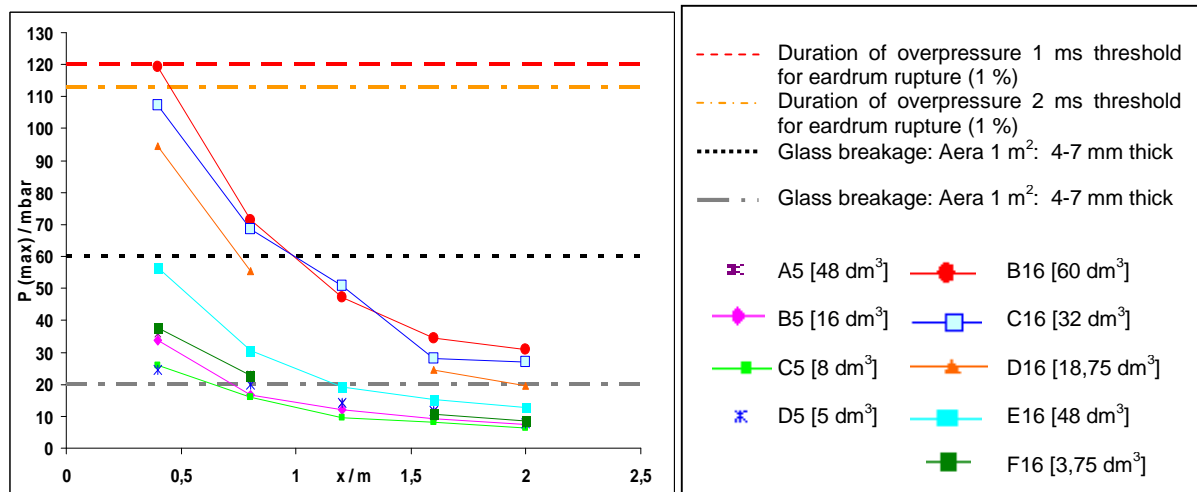


Figure 15: Hazard potential due to peak overpressures from ignited hydrogen releases from the vessels with an initial pressure of 5 and 16 bar.

### 4.2 Possible hazard potential from thermal loads

An early ignition of the released hydrogen close to the nozzle will produce the highest thermal loads, since almost the complete effusing hydrogen is burned and the combustion duration extends over the whole effusion time. Due to the relatively short effusion times of 30 ms to 360 ms for the vessels investigated in this work the diffusion flame generated can be characterised as a blowpipe flame with very high thermal peak capacity. Considering the effusion time of the hydrogen from the vessels as maximum combustion duration of the released hydrogen, and thereby as maximum exposure time of the thermal energy, from the extrapolated data [4] for every vessel the thermal load which may lead to second degree burns can be determined. The intersection of these vessel specific thermal load energies with the linear maximum possible thermal loads on the jet axis in a distance to the nozzle, depicted in Figure 14, produce a vessel specific critical distance on the jet axis. In Figure 16 the critical distances to the nozzle gained with this method are shown for possible second degree burns of human skin versus the released hydrogen amount. The data in Figure 16 show, that for released hydrogen amounts from approx. 4 dm³ to 20 dm³ the critical distance increases rapidly from approx. 50 cm to 200 cm. With a released hydrogen amount of 60 dm³ from vessel B16 the conservatively estimated critical distance for second degree burns of the human skin is 250 cm. Even with 20 liters it is still 200 cm.

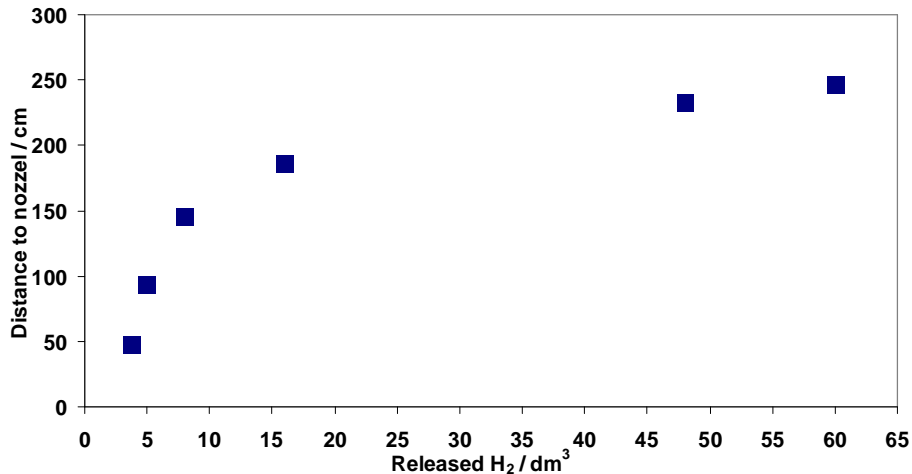


Figure 16: Critical distance to the nozzle for possible second degree burns of human skin.

## 5.0 SUMMARY

In this study unsteady free hydrogen jets from a 10 mm pipe were simulated experimentally. In the experiments hydrogen amounts up to 60 STP dm<sup>3</sup> at initial pressures of 5 and 16 bar were released. The release behaviour of the hydrogen from the facility constructed for the experiments was investigated experimentally and described theoretically. Hydrogen effusion times of 30 ms to 380 ms were measured. Maximum hydrogen release rates of 24 g/s and 97 g/s were determined for the initial pressures of 5 bar and 16 bar, respectively. The free hydrogen jets were ignited by varying ignition position and ignition time delay. The generated pressure waves and thermal loads were investigated systematically. The region with flammable hydrogen mixtures ranges from 1.5 m from the nozzle for small hydrogen amounts and up to 2.5 m for the largest hydrogen amounts investigated. The time span for a possible ignition is in the range of the release time. For every given amount of hydrogen a distinct ignition time and ignition position exists for the generation of a maximum pressure wave due to a "local explosion" in the free jet. The measured side-on overpressure amplitudes at a distance of 40 cm to the explosion origin were between 24 and 120 mbar. The mean duration of the positive pressure phase amounts to approx. 1.5 ms. The possible hazard potential due to pressure waves from the ignited transient H<sub>2</sub> free jets was evaluated in terms of eardrum ruptures. A free jet that is ignited early and close to the nozzle generates the maximum thermal load for its ambience. The combustion duration of the released hydrogen lies in the range of the effusion times. The maximum integral heat flux measured on the jet axis decreases almost linearly with increasing distance to the nozzle. Close to the nozzle thermal loads of 240 kJ/m<sup>2</sup> (initial pressure 5 bar; 48 dm<sup>3</sup>) to 22 kJ/m<sup>2</sup> (initial pressure 16 bar; 4 dm<sup>3</sup>) were measured. The possible hazard from burning of transient H<sub>2</sub> free jets concerning their thermal loads was evaluated for the example of second degree burns of the human skin. In this case the critical distances can reach up to 2.5 m, depending on the released hydrogen mass.

## REFERENCES

1. Zierp, J., Grundzüge der Strömungslehre, 1990, Braun, Karlsruhe.
2. Richmond, D.R., Fletcher, E.R., Yelverton, J.T. and Phillips, Y.Y., Physical correlates of eardrum rupture, *Ann. Otol. Rhinol. Laryngol.*, **98**, 1989, pp. 35–41.
3. Baker, W. E., Cox, P. A., Westine, P. S., Kulesz, J. J., and Strehlow, R. A., Explosion Hazards and Evaluation, 1983, Elsevier Scientific Publishing Co., Amsterdam, The Netherlands.
4. Stoll, A.M., Chianta, M.A., Method and Rating System for Evaluation of Thermal Protection, *Aerospace Medicine*, **40**, 1968, pp. 1232-1238.